Western Michigan University

ScholarWorks at WMU

Paper Engineering Senior Theses   Chemical and Paper Engineering

4-1995

Coat Weight Predictions on the Cylindrical Laboratory Coater

Jared G. Glover
Western Michigan University

Follow this and additional works at: https://scholarworks.wmich.edu/engineer-senior-theses

Part of the Wood Science and Pulp, Paper Technology Commons

Recommended Citation

Coat Weight Predictions on the Cylindrical Laboratory Coater

By

Jared G. Glover

For
Dr. Brian Scheller
Paper 473: Senior Design Problem II
April 13, 1995

A thesis submitted in partial fulfillment of
the degree of Bachelors of Science in
the Department of Paper Science & Engineering
at Western Michigan University
in Kalamazoo, Michigan.

ABSTRACT

Paper Coating attempts to create a smooth and even surface for improved optical and printing sheet performance. Trials were conducted using a blade application on a Cylindrical Laboratory Coater. Two different blade extensions were analyzed. These extensions were key variables that influenced blade forces.

Currently, to achieve a range of coat weights on a sheet, only the trial and error method is performed during a run. The future goal in mind was to have a computer simulation that could make predictions of coat weights without performing the actual trial. This study was conducted to lay the groundwork for future analysis in hope of achieving this long range goal.

A modeling technique was used to relate actual data to predictive data. From this technique, a positive correlation existed between actual data and modeling expectations. The best correlation was due to highly constrained geometries resulting from high run-in settings over the small blade extension. For future study, it is quite possible to establish a computer simulation technique, but it would have to be paper substrate specific and require numerous trials to eliminate all deviations.

TABLE OF CONTENTS

INTRODUCTION

Paper coating is the process of applying a suspension of dispersed particles to create a smoother, more uniform sheet, which improves optical and printing sheet performance. Using a blade to apply the coating formulation, trials were conducted on a Cylindrical Laboratory Coater (CLC). The coat weight values produced were utilized in a modeling technique attempting to achieve predicted results for additional trials. The key parameter that was altered for study was blade deflections due to increased blade forces at the point of application. This was empirically determined from two separate blade extensions. By defining and measuring all variables associated with blade coating, an expected coat weight model was established through three equations associated with three separate forces acting on the system.

The trials were conducted in the Paper Science and Engineering Department at Western Michigan University on the CLC 6000. The short range goal was to establish a basic building block for future study. Eventually, a computer simulation might be developed from the defined model that would eliminate trial and error procedures for attaining specific coat weight ranges.

BACKGROUND

To achieve a better understanding of this thesis, it is important to explain a number of other concepts related to coating, such as:

- Fluid rheology (the study of matter's flow characteristics)
- Hydrodynamic lubrication theory
- Blade coating mechanics
- Structure of coating particles
- Cylindrical laboratory coater operation principles
- Forces related to the CLC

The hydrodynamic lubrication theory results because a fluid develops pressure when moving through a narrowing structure.

Fluid Rheology

To begin with, predicting future reactions of a flowing material is best analyzed under a large range of changing shear (deformation) rates. First, a low shear rate determination of viscosity was performed using a Brookfield viscometer. Second, a larger range was tested using a Hercules Hi-shear viscometer (HHSV). It displays the shear or deformation rate's dependency on its viscosity. This is termed the relationship of shear stress (manipulations) as a function of the shear rate (deformations). Because all methods involve a range of stresses and various other dependent variables (time and flow magnitude), there is no absolute value to a fluid's rheology. Consequently, there are other testing procedures that use higher shear stresses to actually measure capillary effects in the coating formulation with stress levels reaching 10^7 1/seconds. During a coating application stresses under the blade are known to exceed even that level. Roper and Attal (1993)[1] measured those parameters

on different coating formulations. However, these high stress levels were not evaluated for this study.

There are some terms that describe a fluid's response to shear that must be fully defined. The Hercules Hi-shear viscometer (HHSV) displays the response in graphs called rheograms: two axes graphs, plotting increasing rpm versus changing torque. The plotted curves are generated as the testing cycle begins at zero rpm and accelerates to the maximum tested rpm and then back to zero. The geometric shape of those rheograms portray the fluid's rheology. *(The actual rheogram for the tested coating formulation is shown in the RESULTS Section of the text.)*

There are three major categories for fluid behavior: Newtonian, time dependent behavior, and shear dependent behavior. A coating formulation often exhibits a number of these behaviors throughout a full range of different stresses. In 1989, Triantafillopoulos[2] described the basic fluid measurements and interpreted the resulting rheograms.

First, a Newtonian fluid behaves under the exact expectations of Newton's laws of physics, such that, there is no change in the liquid from increasing or decreasing force. This principle follows Newton's law that for every action there exists and equal and opposite reaction. The rheogram shows this in a linear plot, in which, the increasing and decreasing rpms travel along the identical pathway *(See FIGURE 1)* .

Second, the time dependent phenomena contain two opposing behaviors: thixotropy and rheopexy (anti-thixotropy). A thixotropic fluid undergoes a catastrophic breakage in its internal structure from

increasing force, and structural reformation occurs during the decreasing force cycle. Thixotropy is defined as an isothermal, reversible reduction in viscosity with a sensitivity to the history of the previous shears incurred on the fluid. Graphically, a loop is created by a curved pathway as torque increases faster than rpms, and then on the down cycle, an almost straight pathway, similar to the Newtonian rheogram, occurs *(See FIGURE 2)*. On the other hand, a rheopexic fluid has an identical rheogram as a thixotropic fluid, however, the increasing stage and decreasing stage are reversed. The same loop forms as rheopexy is defined as an isothermal, reversible viscosity increase with shear rate. This opposing phenomenon occurs because an internal structure forms from increasing particle collisions under shear *(See FIGURE 3)*.

Figure 1.
Newtonian Fluid
Rheogram

Figure 2.
A Thixotropy
Rheogram

Figure 3.
A Rheopexy
Rheogram
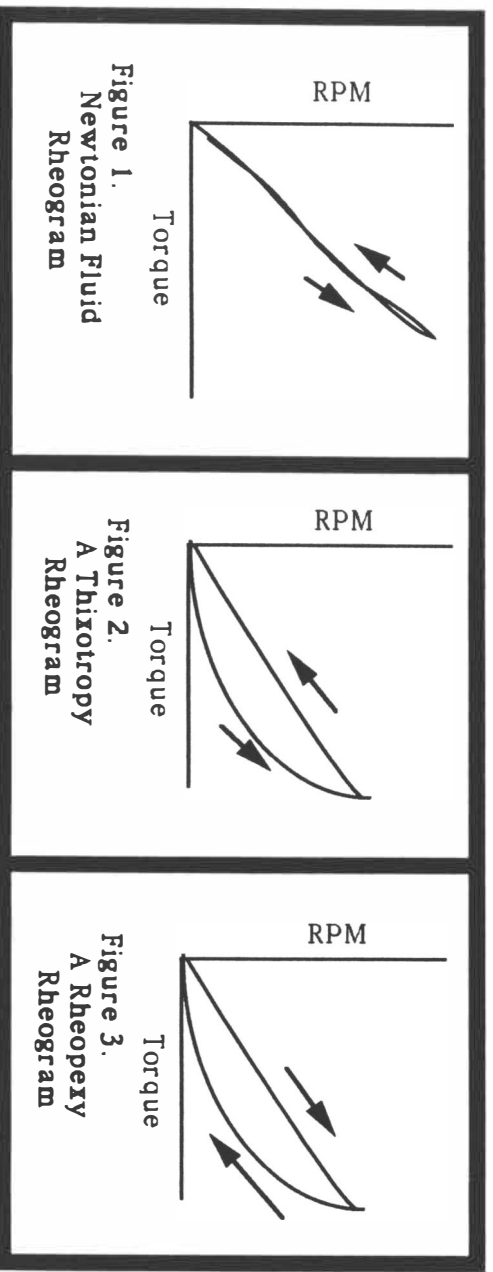
Third, shear dependent phenomena can be grouped into three categories: shear thickening (dilatancy), shear thinning (pseudoplasticity), and plasticity. To begin with, shear thickening is an isothermal, reversible viscosity increase as a function of shear rate. Under normal flow, voids are created and filled by particles

sliding against one another, but dilatancy occurs when those voids are no longer created, only filled. This makes the fluid act similar to a solid as it resists flow in the same manner. On the rheogram, a convex line is characterized by a large non-maximizing increase in torque (*See FIGURE 4*). Often, the opposing force created is too high for the test range to be completed. Next, psuedoplastic or shear thinning behavior has a similar curve as thixotropic phenomenon but concave in shape. A maximum torque is not achieved because the fluid flows more easily with increased torque. This occurs as viscosity decreases with shear rate as both the chemical primary and secondary bonds holding the fluid together, are easily broken under the shear effects (*See FIGURE 5*). Moreover, a fluid may exhibit a plastic behavior, which is defined as movement only after a critical level of shear is exceeded. The rheogram increases in torque without any rpm increase as shear develops to reach that critical level (*See FIGURE 6*). Finally, it is important to realize that fluids may demonstrate a combination of all these behaviors over a variety of shear ranges.

RPM

Torque
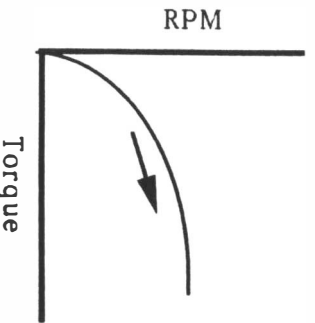
Figure 4.
Shear Thickening
or a Dilatancy
Rheogram

RPM

Torque
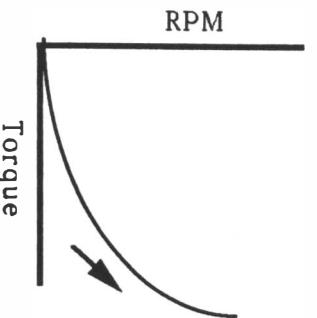
Figure 5.
Shear Thinning or
a Pseudoplasticity
Rheogram

RPM

τ_c

Torque

τ_c -Critical Torque
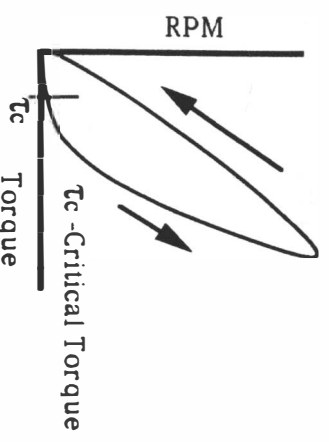
Figure 6.
A Plasticity
Rheogram

Hydrodynamic Theory
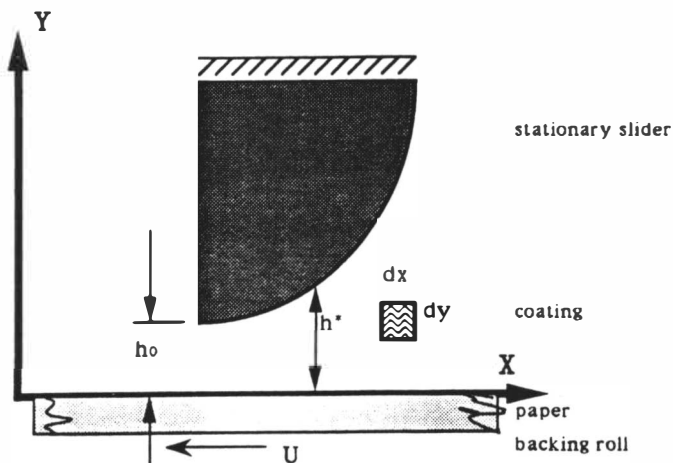
Figure 7. A Generalized Narrowing Geometry or Fluid Wedge
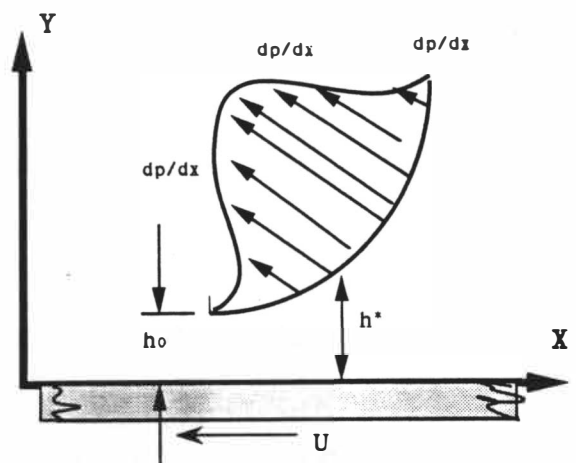
Figure 8. The Pressure Profile of the Fluid Wedge from Figure 1.

Next, the hydrodynamic theory, originated in 1889 by Osborne Reynolds, must be understood to comprehend the principles of a paper coating. Bliesner (1971)[3] states that when a stationary slider (a curved or slanted surface that is rigidly fixed and immobile) forms a converging channel or pathway with respect to a moving member, and a fluid occupies that intervening pathway, there exists a pressure distribution generated in that pathway or fluid wedge *(See FIGURE 7 & 8)*. For a machine coater, the stationary slider is the blade, the moving member is the backing roll's velocity transferred to the paper substrate, and the fluid is the coating formulation.

There are some basic assumptions that must be incorporated for the theory to hold. The fluid must:

- Exist with laminar flow conditions.
- Behave according to Newtonian principles, thereby being unaffected by shear rate.
- Be incompressible.
- Only generate a single directional force (x) with respect to force and velocity parameters.
- Have a velocity as a two dimensional function (both x and y).

Now that the theory has been visually presented, it can be expressed mathematically:

Equation 1:

$$\frac{dp}{dx} = 6\mu U \left(\frac{h^* - h}{h^2}\right)$$

Where:

dp/dx	=	pressure gradient at any point along the wedge
μ	=	fluid viscosity
U	=	velocity of paper (backing roll velocity)
h	=	separation between the fixed and moveable surface at any horizontal point, x.
h^*	=	thickness of final fluid film (after the wedge)

From the results of Equation 1 and figures 7 & 8,
at the exit of the wedge where there is no pressure p = 0,
but dp/dx = + value,
        $h = h_o$
at the maximum pressure, dp/dx = 0,
        $h = h^*$
at entrance of the wedge, where p = 0 and dp/dx = 0,
        $h > h^*$

The described assumptions are fairly typical for fluids, however, most coating formulations have a non-Newtonian behavior, which causes some limits to the application of the hydrodynamic theory to the blade coating process. For example, Windle and Beazley (1967)[4] studied these restrictions for coating formulations and discovered that most demonstrate a shear-thinning principle. Therefore, the coating would produce a higher blade thrust, (the force developed through blade characteristics), as compared to an even thrust produced with a Newtonian fluid. They concluded that the difference in the fluid's property did not affect the calculations significantly. However, this is not always the case. Therefore, the

non-Newtonian behavior cannot be too deviant, or this theory does not work as expected.

As described previously, the shear-dependent behaviors produce the most significant prediction errors. If thixotropic or rheopexic behaviors are severe enough, then prediction errors can also arise, but more likely runnability problems would be more prevalent. According to Roper and Attal (1993), the second most important coater runnability problem is colloidal and shear instabilities in the coating formulation. Examples of such problems would be inability to control coat weights, scratching marks on the sheet, and excessive build up of pigment behind the blade. From their work, it was desirable to minimize the blade pressures, which would help even blade wear because a wide range of shear rates are experienced under the blade during very short dwell times. Those rates can exceed 1×10^6 1/second, therefore, knowledge of the high shear behavior of the coating are quite beneficial. In addition, their study also noted that basestock parameters, absorbency and roughness, affected the coating results. For this reason, Lyons (1989)[5] accounted for such alterations in his coat weight model.

Roper and Attal (1993) found that a small latex particle reduced dilantant effects under increasing shear. If, however, the solids were increased that dilatant behavior increased in the formulation. It is important to minimize any dilatant behaviors as they will create high blade pressure due to hydrodynamic forces and cause severe runnability problems *[See blade coating mechanics section for additional information about Roper and Attal's (1993) work].*

Coating Particle Structures

The majority of the coating formulation consists of pigment particles. For my analysis, the pigment was Number 2 kaolin clay particles. The classification refers to average particle size. From the information by Gill and Hagemeyer (1994)[6], the clay particle's structure is plate-like and exhibits a net anionic charge when dispersed in water, even though the individual molecules are amphoteric, having both positive and negative charge. The negative charge is associated with the surface and the positive charge with the outer edge. Because of the small size, each particle has a large surface area which accounts for the net negative charge when dispersed. The latex particles are the binder particles. They aid in binding the clay to other particles including the paper fines and fibers. The even spherical structure of latex particles helps fill voids created from the plate stacking that occurs with clay. Next, alcogum is added to thicken the mixture for application. Proper pH is maintained for proper chemical stability. Finally, to achieve the desired consistency (lowering the solids content), dilution occurs with water.

Water Retention of Coating

An important aspect of coating is the dewatering of the formulation from the interaction of paper to liquid when the two contact. To measure this principle, the actual amount of water, (penetrated into the substrate after passing through a filter under an external pressure for a specified time duration), is weighed and converted to basis weight values. This is accomplished by using the Åbo Akademi Gravimetric Water Retention Meter (ÅAGWR). The

filter used has a small, well defined pore structure (0.8 µm Millipore filter pads). Termed the gravimetric method by Sandas, Salminen, and Eklund (1989)[7], its direct quantification of the aqueous phase lost to the absorbing substrate is its key advantage over other indirect water retention analysis.

From intuition, results can be predicted. Clay particles tend to hinder liquid transfer by plugging filter pores from their plate-like structure. High solids has less water to contact the sheet, therefore, less free molecules for removal. These two reasons would cause less coating to penetrate into the sheet. For a full spectrum of the formulation's performance, contact times should be varied along with external pressures. Currently, there is no quantifiable application into this coat weight modeling procedure, however, the analysis does produce information to better understand liquid-sheet transfer.

Blade Coating Mechanics
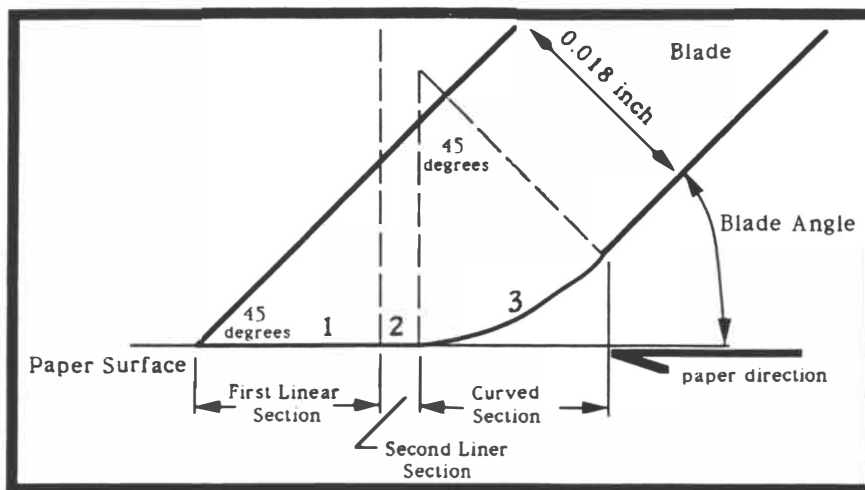
Figure 9. The Blade Tip Model

Blade Coating has been established as the most popular and stable form of coating application through the years. It's known that

coat weights are due to the forces generated by the hydrodynamic actions at the blade and additional forces applied to the operating conditions. The blade contacts the paper to optimize an even "land" contact across the paper surface, which maximizes surface contact to achieve even wear across blade, hence smooth application *(See FIGURE 9)*. There are three regions necessary with a blade tip, the first linear region, the curved region forming a slider edge, and the second linear region initiating contact again with the sheet at the prescribed angle.

An even "land" placement of the blade is utilized to minimize runnability problems like whiskering and weeping, the build up and drying of coating pigment on edges of the blade that create unwanted streaks and deposits on the sheet's surface. These are time dependent problems that cannot be analyzed on a CLC because of the short application (run) time *(Branston, Clark, Errico, Scriven, Sheehan, Suszynski, Takamura, and Vodnick (1994) studied these effects on production equipment).*[8]

Using the equation described previously *(Hydrodynamic Theory Section: Equation 1)*, and the geometry of the blade tip, the pressure distribution can be calculated. From this analysis, accurate predictions can be generated. However, there are some key complications that effect the analysis. To begin with, the actual angle does not precisely equal the set value known at the zero point (the tangential point of contact with the blade and the backing roll). The angle becomes smaller as force is increased causing the blade to deflect. This blade force is a required parameter to directly alter coating weight. More blade force pushes against the paper surface

and lowers the resulting coat weight. This effect has been quantified *(discussed later in the Force Analysis for the CLC section)*.

Moreover, a significantly larger complication surfaces from the compressibility of the paper, the backing roll, and the resulting fluid thicknesses of the applied coating. Empirically, the compressibility has been related to the blade angle, such that a more compressible base produces a higher angle. These effects have been accounted for by Lyons (1993) through his calculations and the backing roll properties. It is important to know these parameters to establish a model for analysis.

Now that a model has been defined, the application of the hydrodynamic theory leads to a value for the pressure distribution resulting from the fluid wedge under the blade. The final fluid film thickness, h^*, is:

$$h^* = W/ \chi \rho$$

where,

W	=	Coat Weight
χ	=	Solids percentage of the coating
ρ	=	Coating's density

Even though this is quantifiable, the actual position that this occurs is not known, but some location on the x axis *(refer to FIGURE 7, above)*. However, the final film thickness, h_o, at the wedge outlet is less than the outlet thickness, h^*. A relationship has been developed to fix the position of h_o through the use of a gain constant, C_i, such that:

$$h_o = C_i(h^*).$$

Through assumption of a values relating fixed geometry and the pressure distribution, Bliesner (1971) and Lyons (1993), utilized

mathematical trial and error analysis to establish the accurate conditions for film thickness and location.

Furthermore, it is imperative that one looks at the blade through logical analysis. For instance, one expects that coating weight will influence the pressure distribution. Bliesner (1971) agreed that lower coat weights allow higher pressures to be produced near the blade tip, whereas, higher coating weights give a more dispersed, broad pressure distribution. Accurate hydrodynamic considerations will produce good modeling of blade coating.

These principles were utilized by Roper and Attal (1993) when analyzing pilot coater results through both blade mechanics and coating rheology. To achieve a more accurate production simulation, these researchers ran at high speeds, 3500 ft/min. Their trials attempted to maintain a "clean" and uniform blade to produce good coat weight control without the use of high blade pressures. High blade pressures increase the frequency of sheet breaks causing a production time loss. Consistent and reproducible data resulted from a controlled blade geometry by utilizing coating rheological properties, durable ceramic blades (reducing uneven wear), and known blade thicknesses, angles, and machine speeds. Through the analysis of rheology and blade mechanics, the hydrodynamic forces can thoroughly be predicted, leading to better coat weight control.

Cylindrical Laboratory Coater (CLC) Description

The main purpose of the CLC is to simulate the coating mechanism of a machine coater. This demonstrates behavioral characteristics of the coating formulation, but is limited because it is

not the exact production equipment. Therefore, time dependent runnability problems do not occur. However, it does serve the machine simulation purpose and uses minimal personnel with no lost production time by using the machine coater. There are a number of variables that the CLC utilizes: altering machine speeds, dwell times (the time period that the coating pigment contacts the paper surface, prior to the doctoring or scraping off action of the blade), blade characteristics, preheating conditions, and drying environments.

Suwala and Ottone (1992)[9] have conducted numerous CLC runs to minimize product deviations and define expectations from varying the previously mentions variables. To validate their results, target coat weights were produced on the CLC. This is necessary when studying the final optical properties of the sheet for proper comparison. Micrometer settings were altered to achieve the desired coat weights during each variable change. This change alters the blade force (F_b as defined by Lyons (1993) *See next section -- Force Analysis for the CLC*). At higher speeds, blade thickness and pond dwell time influenced the process more dramatically causing larger variations in the micrometer (run-in) settings to achieve target coat weights. In addition, thicker blades and shorter dwell time required less run-in (blade) force.

Force Analysis for the CLC

Now that the basics have been introduced, one can look at the actual forces that will occur at the blade. There are three forces acting on the system during blade coating: hydrodynamic force, loading force (commonly called blade force), and inertial force as defined by Lyons (1993) *(See FIGURE 10)..*
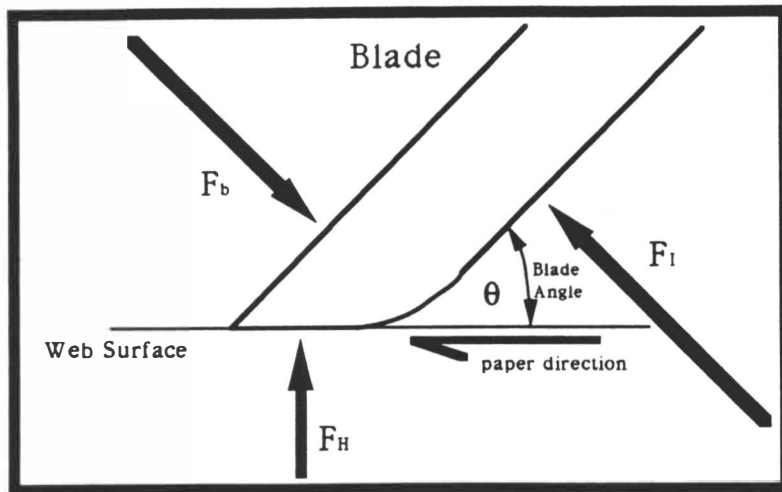
Figure 10. Forces Acting at the Blade

Blade Force

First, the loading or blade force can be calculated. The force is related to the run-in (pressure generated by the micrometer setting), and stiffness of the blade *(See FIGURE 11)*. The run-in, or micrometer setting, is used to control the coating weight, more force reduces coating. During the set-up stage, the blade is set to zero point while the backing roll is stationary, but preheated. This zero point is established as the exact point the blade touches the backing roll surface. By increasing the micrometer reading, it moves the blade beyond the zero point and into the backing roll. However, while the system is in operation the force developed by the flowing fluid causes the blade to move *(Refer to Hydrodynamic Force discussed later)*. This all occurs at speeds of two thousand plus feet per minute at contact points measured in thousandths of an inch. Now, it is quite understandable why there are so many questions, the blade geometry changes and the backing roll deforms while compacting the substrate and coating.

Stiffness of the system is a function of the blade and the backing roll parameters.   It is calculated to be:

$$S = \left[\frac{4 L^3}{E_B b^3 W} + \frac{t (1 - v_R^2) \sin \theta}{W b E_R} \right]^{-1}$$

$S_{final} =$ $S / \cos \theta$, this transfers the value to the Y-direction.

the variables are:

L   -   Extension of Blade
b   -   Thickness of Blade
E_B -   Elastic Modulus of Blade
W   -   Width of Blade
t   -   Thickness of Backing Roll
v_R -   Possion's Ratio
θ -   Angle of Blade
E_R -   Elastic Modulus of Backing Roll

All distances are in inches and angles are in radians.

The Run-in (convert to inches) relates so that, $F_B = (\delta) (S_{final})$.
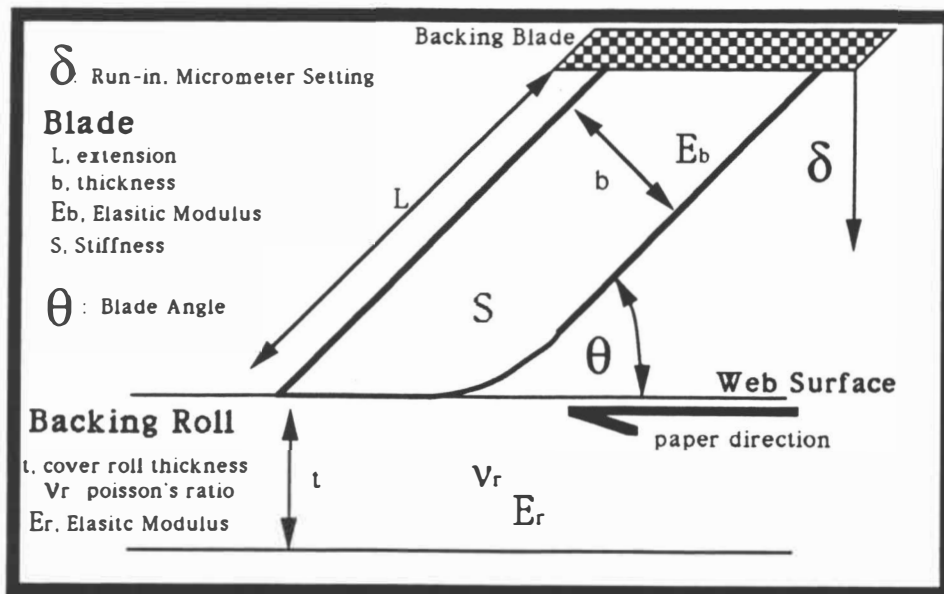
Figure 11. Blade Force Parameters

Hydrodynamic Force

Second, the hydrodynamic force is a direct application of the previously mentioned theory *(Refer to Hydrodynamic Theory)*. It relates the blade geometries, machine operations, and the coating's properties to the expectations of fluid flow through narrow geometries *(See FIGURE 12)*.

$$F_H = \frac{6 \eta S^2 U W}{H^2} [1-2(H^*/H_0)]$$

where, $2(H^*/H_0) = k$
        is a scaling factor defined by hydrodynamic theory
η -   Viscosity
S   -   Stiffness of the Blade
U   -   Machine Velocity
W   -   Width of the Blade
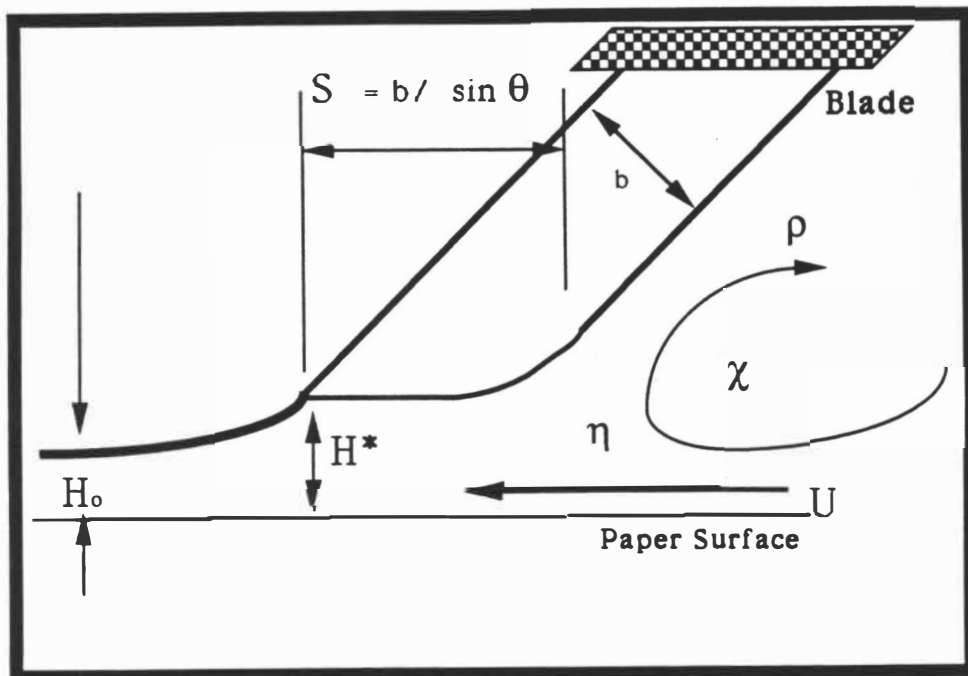
Figure 12. Hydrodynamic Force Parameters

From substitution

$$F_H = \frac{6\eta S^2 U W (1-k) k^2}{4 H_w^2}$$

where, η is proportional to Brookfield viscosity, B, and other terms can be grouped, so that:

$$\mathbf{F_H} = \frac{\beta^2 \mathbf{B S^2 U W}}{\mathbf{H_w}^2}$$

β is function of k, h/B; $= \dfrac{6\eta(1-k)k^2}{4}$

Since, one cannot measure the distances of H or H_w during operation, they must be estimated from mathematical analysis. Unknown terms can be grouped together with constants because of the proportional relationship.

Inertial Force

Third, the inertial force relates expectations of the flowing fluid and its characteristics to the stationary blade structure. In simple terms, it accounts for the changing direction of flow impacting on the blade and the sheet *(See FIGURE 13)*.
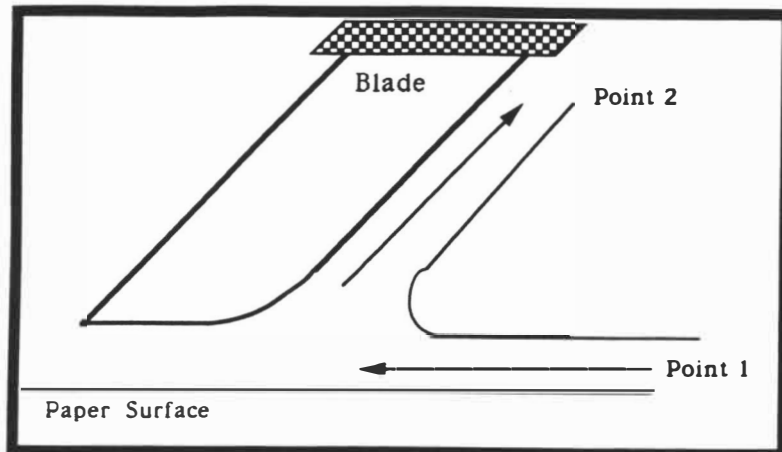
Figure 13. Inertial Force Parameters

Initially, start with Bernoulli's equation:

$$\frac{(v_1)^2}{2} + \frac{(p_1)}{\rho} + \frac{(gh_1)}{} = \frac{(v_2)^2}{2} + \frac{(p_2)}{\rho} + \frac{(gh_2)}{}.$$

Point 1 & 2   (characterized by subscripts)

v   -   velocity
p   -   pressure
ρ -   density
g   -   gravity constant
h   -   height

Assuming that Point 2 is a stagnation point and there is no height difference from point to point, the equation becomes:

$$\frac{(v_1)^2}{2} = \frac{(p_2 - p_1)}{\rho}$$

The definition of impact force given as $F_I = Wh(p_2 - p_1)$. Height, h, does have an effect on impact force, but it is indeterminable. Therefore, it's grouped along with the proportion of fluid velocity to machine speed, U, into unknown quantity, γ. So that, $\mathbf{F_I = \rho\gamma U^2}$.

Coat Weight Model

Finally, one must relate all three forces together by summing in the Y-direction. Therefore, $\mathbf{F_I + F_H - F_B\cos\theta = 0}$. Substitution of the above equations yields:

$$\mathbf{F_B\cos\theta} - \frac{\beta^2\mathbf{B S}^2 \mathbf{W}}{\mathbf{H_w}^2} - \rho\gamma U^2 = 0$$

Through rearrangement, the wet coating thickness can be solved.

$$H_w^2 = \left[\frac{\beta^2 B S^2 UW}{F_B\cos\theta - \rho\gamma U^2} \right]^{1/2}$$

Intuitively, the coat weight is the wet coating thickness times both solids and density plus the minimum coat weight (the amount required to simply fill the tiny voids to create an even surface). Therefore, the model becomes:

$$CW = CW_0 + \rho\chi * \left[\frac{\beta^2 B S^2 U W}{F_B \cos\theta - \rho\gamma U^2} \right]^{1/2}$$

From this analysis, Lyons (1993) further grouped terms to simplify the model by a necessary conversion factor (475,200 converting $inch^2$ to reams) *(Refer to PROCEDURE section complete equations)*.

EXPERIMENTAL PROCEDURES

Coating Formulation

Ingredients	Concentration	Solids	Wet Weight	Totals(dry)	Totals
	parts/hundred	%	grams	grams	wet
#2 Kaolin Clay	100	72	138.8	3100	4300
(pigment)					
Styrene Butadiene Latex	16	50	32	496	992
(binder)					
Alcogum	1.5	35*	1.5	-	45
(thickener)					

* add- "as is", manufacturer has already accounted
for solids, just determine concentration and use that value.

pH: 8.5 (Adjusted with NaOH)   Total Solids: 67.8%
Viscosity (cP):   1220   Diluted Solids: 60.25%

Actual Formulation Procedure
1)   Values to make approximately 4 L of coating *(see Appendix I)*
2)   All weighted values performed with balance accuracy +/-0.5 g.
2)   Dispersed Clay with disperser and water
.3)   Under a mixer, added Latex
4)   Set to desired pH, 8.5
5)   Added Thickener
6)   Diluted, checked for solids
7)   Achieved targeted range 60% (+/- 0.5)
8)   Sealed Container, Stored in Walk-in Cooler.

Errors

•   Should have only added 0.5 pph of alcogum, instead through miscalculation
    of "as is" condition, 1.5 pph of alcogum totaling 45 g. was added.

•   Additional diluting with water was performed to lower solids to 60%

Hercules Hi-Shear Viscometer Test performed and rheograms were
made.

CLC Procedures

1) Removed Coating from Cooler, Removed Top Dried Layer
2) Placed Under Mixer, Rechecked Solids to Verify
3) Coating Formulation Continuously Mixed During Trial
4) Cleaned Blade & Carriage Apparatus
5) Set-up Blade Configuration--using thick backing blade-1/4 inch
   a) Measured Extension, Thickness, Width with Calipers
   b) Measured Backing Roll Thickness with Calipers

6) Attached Carriage Apparatus
7) Closed Safety Covering
8) Set Speed, 2000 fpm
9) Warm up, no coating Runs (6)
10) Set Zero Point With Blade to Backing Roll Contact

11) Attached One Revolution Strip of Paper to Backing Roll w/ Tape
12) Dialed Micrometer to Desired Setting (5-50: 1/1000 inch)
13) Poured Coating Formulation into Pond to Specific Level
14) Replaced Coating Under Mixer
15) Closed Safety Covering and Pushed Start Button

16) CLC Operation
    a) Desired Speed Achieved
    b) Heating Elements Heated Sheet
    c) Pond/Blade Apparatus Laterally Applies Coating to the Sheet
    d) Heating Elements Dry Coating
    e) Shuts off, Apparatus Transfers Laterally Back to Starting Point
17) Opened Safety Cover, Remove Pond/Blade Apparatus
18) Poured Unused Coating into the Mixing Coating
19) Cleaned Pond/Blade with Water/Scrubber
20) Removed Coated Sheet

21) Cut Small Section of Original Paper for Base Sheet Comparison
22) Cut Sample of Coated Sheet
23) Cut Circular Samples-- Both Sheets Simultaneously, cover same area
24) Placed Samples Separately in Microwave at Lower Power--75%
25) Obtained Original Dry Weight of Each Sample

26) Calculated Approximate Coat Weights from Values (Coated-Base)
27) Saved Samples for Coat Weight Verification After Trials
28) Attached New Sample, Dialed New Micrometer Setting,
    Began Next Trial

Coat Weight Verification

Simply Performed Original Method with Microwave. The main goal was to make enough numbers to obtain average values and disregard both high and low numbers.

It is possible to determine coat weights through an ash testing technique, but this was not performed because precision was not necessary for modeling.

Water Retention Testing *(Refer to FIGURE 14 & 15)*

1) Set up Apparatus by Attaching Pressure Line to Inlet Air
2) Lift Upper part of knob B, turn counter-clockwise until it stops
3) This Sets Pressure to Work Between 0-0.6 bar (IMPORTANT)
4) Cut Sample Blotting Paper (approx. 60 mm X 60 mm squares)
5) Turn Switch C to OFF

6) Turn on Pressure with Knob B--Lift Knob Turn Clockwise until Desired Pressure is Obtained.
7) LOCK Knob B (a variety of pressures are desired for analysis)
8) Note Pressure after lock (it may drop)
9) Weigh Cut Blotting Paper Sample--note weight
10) Place it on the Small Rubber Covered Table

11) Place a Nuclepore filter (or other filter paper) on Blotting Paper
12) Place the Metal Cup on Filter
13) Place the Whole Table/Papers/Cup Combination on Instrument Table, so that the Cup Will Rest Against the Metal Pins.
14) Turn Switch D to Raise the Cup
15) Pour Coating into Cup Using a Pipette, <u>Quickly</u> Screw ON Cover

16) Turn SWITCH C to ON position. . .pressure is then set
17) Start Watch, Account for Delay Time (approx. 8 seconds)
18) Measure & Note Desired Length of Time (again variety is good)
19) Release Pressure by Switching C to OFF.
20) Lower Table by Switching D

21) Remove Table Combination
22) Pour Out Excess Coating, Remove Blotting Paper (CAREFUL, this step is very tricky)
23) Re-weigh Blotting Paper--note weight
24) Multiply the Two Weight Difference by 1250 to attain penetrated amount of water in g/m^2.
25) Wash and Dry Cup Before Next Test

Modeling Procedures & Numbers

Presented here is a quick and concise view of the variables utilized in the modeling equations. Also, the acutal and theoritical model will be presented.

<u>Variable List</u>

Blade

Variable		Description	Units	Values
S	-	Stiffness	pound force/ inch	SEE BELOW
L	-	Extension	inch	0.3 or 0.6
b	-	Thickness	inch	0.018
E_B	-	Elastic Modulus	dimensionless	$3 * 10^6$
W	-	Width	inch	5.5
θ	-	Angle	45° to radians	.785398163
δ	-	"Run-in" or Micrometer setting	inches (δ/1000)	.001 to .05

Backing Roll

Variable		Description	Units	Values
t	-	Thickness	inches	0.65
v_R	-	Possion's Ratio	dimensionless	0.5
E_R	-	Elastic Modulus	dimensionless	50,000
U	-	Mach. Velocity	fpm to inch/min	2000: 24,000

Coating Formulation

Variable		Description	Units	Values
η:B	-	Brookfield Viscosity Conversion $(2.4* 2.0886* 10^{-5})$	centipoise to lb/(in* min)	1220 cP 0.06115421
ρ	-	Specific Gravity to Density Conversion $(\rho * 62.4/12^3)$	lb/in^3	1.41 0.0509167
χ	-	Solids	% to decimal	60.25 0.6025

Other Variables

Variable	Description	Values
CW_0 -	Minimum Coat Weight	0.0
k -	Proportionate factor $2(H^*/H_0)$	0.5
Iterative Determined Variables For "Fit" Modeling Technique		
β -	Scaling Factor related to Hydrodynamic Forces	$2.155*10^{-4}$
γ -	Scaling Factor related to Inertial Forces	$5.1 * 10^{-9}$

Calculated Variables

S, Stiffness (lb_f/inch)

$$S = \left[\frac{4 L^3}{E_B b^3 W} + \frac{t (1- \nu_R^2) \sin \theta}{W b E_R} \right]^{-1}$$

$S_{final} = S / \cos \theta$, this transfers the value to the Y-direction.

Therefore since both are in the
Y-direction, blade force becomes: $F_B = (\delta) (S_{final})$

Model Equations

Theoretical
$$CW = CW_0 + \rho\chi * \left[\frac{\beta^2 B S^2 U W}{F_B \cos\theta - \rho\gamma U^2} \right]^{1/2}$$

Actual w/ Conversions
$$CW = CW_0 + (475,200)*\beta*\rho*\chi*(b/\sin \theta) * \left[\frac{B*U*W}{S*\delta*\cos\theta - \rho*\gamma*U^2} \right]^{0.5}$$

RESULTS

Water Retention Test

Sample	Wt. Difference	Time	Pressure	Water Retained
A	0.007 g	2 min.	0.26 bar	8.75 g/m^2
B	0.0087 g	2 min.	0.26 bar	10.875 g/m^2
C	0.028 g	4.5 min.	0.26 bar	35 g/m^2
D	0.0348 g	4.5 min.	0.29 bar	43.5 g/m^2
E	0.0299 g	4.5 min.	0.36 bar	37.375 g/m^2
F	0.0295 g	4.5 min.	0.36 bar	36.875 g/m^2

CLC Trial

Extension inches	blade run-in micrometer	Ave. Coat Wt. g/sq. m.	Ave. Coat Wt. lb./ream
0.3	50	1.85	1.14
0.3	30	2.57	1.58
0.3	20	5.5	3.38
0.3	10	6.9	4.24

Extension inches	blade run-in micrometer	Ave. Coat Wt. g/sq. m	Ave. Coat Wt. lb/ream
0.6	30	6.97	4.28
0.6	20	8.66	5.32
0.6	10	11.34	6.96
0.6	5	17.9	11

Hercules Hi-Shear Tester Data for Formulation

TORQUE Kilodyne-cm

RPM

1-1
GLOVER1-.DAT
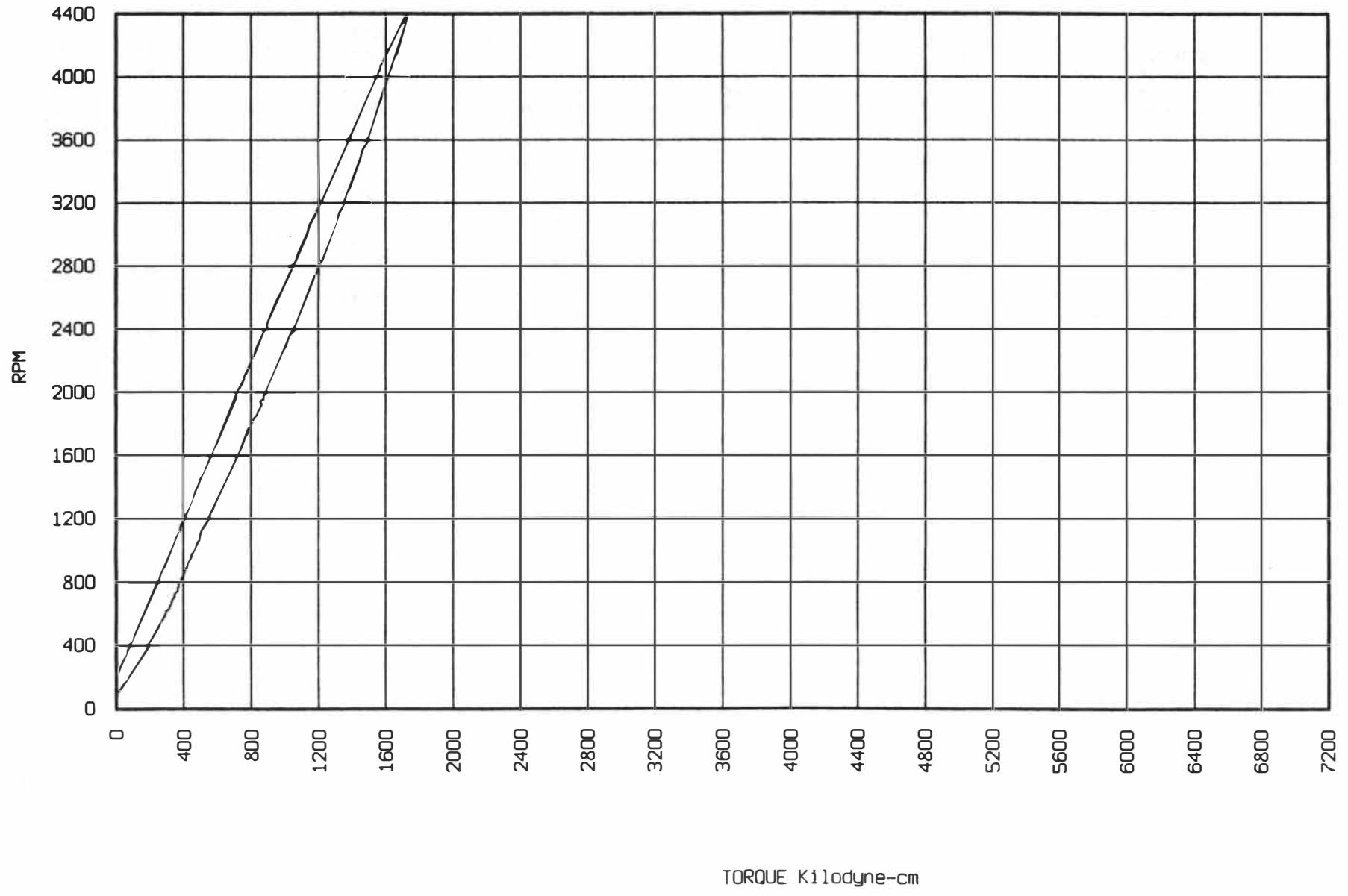
broll-thick,t	oll elast. mod	poisson's ratio	velocity, U	angle	angle	blade thick, b	bl. elasitic mod	bl. width, W	extension, L	S	Final S	Micrometer
inch	Er	v,	in./min	degrees	radians	inch	Eb	inch	inch		S/Cos(angle)	10^-6 Meters
0.65	50000	0.5	24000	45	0.78539816	0.018	3000000	5.5	0.6	110.518	156.295793	1
0.65	50000	0.5	24000	45	0.78539816	0.018	3000000	5.5	0.6	110.518	156.295793	2
0.65	50000	0.5	24000	45	0.78539816	0.018	3000000	5.5	0.6	110.518	156.295793	3
0.65	50000	0.5	24000	45	0.78539816	0.018	3000000	5.5	0.6	110.518	156.295793	4
0.65	50000	0.5	24000	45	0.78539816	0.018	3000000	5.5	0.6	110.518	156.295793	5
0.65	50000	0.5	24000	45	0.78539816	0.018	3000000	5.5	0.6	110.518	156.295793	6
0.65	50000	0.5	24000	45	0.78539816	0.018	3000000	5.5	0.6	110.518	156.295793	7
0.65	50000	0.5	24000	45	0.78539816	0.018	3000000	5.5	0.6	110.518	156.295793	8
0.65	50000	0.5	24000	45	0.78539816	0.018	3000000	5.5	0.6	110.518	156.295793	9
0.65	50000	0.5	24000	45	0.78539816	0.018	3000000	5.5	0.6	110.518	156.295793	10
0.65	50000	0.5	24000	45	0.78539816	0.018	3000000	5.5	0.6	110.518	156.295793	11
0.65	50000	0.5	24000	45	0.78539816	0.018	3000000	5.5	0.6	110.518	156.295793	12
0.65	50000	0.5	24000	45	0.78539816	0.018	3000000	5.5	0.6	110.518	156.295793	13
0.65	50000	0.5	24000	45	0.78539816	0.018	3000000	5.5	0.6	110.518	156.295793	14
0.65	50000	0.5	24000	45	0.78539816	0.018	3000000	5.5	0.6	110.518	156.295793	15
0.65	50000	0.5	24000	45	0.78539816	0.018	3000000	5.5	0.6	110.518	156.295793	16
0.65	50000	0.5	24000	45	0.78539816	0.018	3000000	5.5	0.6	110.518	156.295793	17
0.65	50000	0.5	24000	45	0.78539816	0.018	3000000	5.5	0.6	110.518	156.295793	18
0.65	50000	0.5	24000	45	0.78539816	0.018	3000000	5.5	0.6	110.518	156.295793	19
0.65	50000	0.5	24000	45	0.78539816	0.018	3000000	5.5	0.6	110.518	156.295793	20
0.65	50000	0.5	24000	45	0.78539816	0.018	3000000	5.5	0.6	110.518	156.295793	21
0.65	50000	0.5	24000	45	0.78539816	0.018	3000000	5.5	0.6	110.518	156.295793	22
0.65	50000	0.5	24000	45	0.78539816	0.018	3000000	5.5	0.6	110.518	156.295793	23
0.65	50000	0.5	24000	45	0.78539816	0.018	3000000	5.5	0.6	110.518	156.295793	24
0.65	50000	0.5	24000	45	0.78539816	0.018	3000000	5.5	0.6	110.518	156.295793	25
0.65	50000	0.5	24000	45	0.78539816	0.018	3000000	5.5	0.6	110.518	156.295793	26
0.65	50000	0.5	24000	45	0.78539816	0.018	3000000	5.5	0.6	110.518	156.295793	27
0.65	50000	0.5	24000	45	0.78539816	0.018	3000000	5.5	0.6	110.518	156.295793	28
0.65	50000	0.5	24000	45	0.78539816	0.018	3000000	5.5	0.6	110.518	156.295793	29
0.65	50000	0.5	24000	45	0.78539816	0.018	3000000	5.5	0.6	110.518	156.295793	30
0.65	50000	0.5	24000	45	0.78539816	0.018	3000000	5.5	0.6	110.518	156.295793	31
0.65	50000	0.5	24000	45	0.78539816	0.018	3000000	5.5	0.6	110.518	156.295793	32
0.65	50000	0.5	24000	45	0.78539816	0.018	3000000	5.5	0.6	110.518	156.295793	33
0.65	50000	0.5	24000	45	0.78539816	0.018	3000000	5.5	0.6	110.518	156.295793	34
0.65	50000	0.5	24000	45	0.78539816	0.018	3000000	5.5	0.6	110.518	156.295793	35
0.65	50000	0.5	24000	45	0.78539816	0.018	3000000	5.5	0.6	110.518	156.295793	36
0.65	50000	0.5	24000	45	0.78539816	0.018	3000000	5.5	0.6	110.518	156.295793	37
0.65	50000	0.5	24000	45	0.78539816	0.018	3000000	5.5	0.6	110.518	156.295793	38
0.65	50000	0.5	24000	45	0.78539816	0.018	3000000	5.5	0.6	110.518	156.295793	39
0.65	50000	0.5	24000	45	0.78539816	0.018	3000000	5.5	0.6	110.518	156.295793	40
0.65	50000	0.5	24000	45	0.78539816	0.018	3000000	5.5	0.6	110.518	156.295793	41
0.65	50000	0.5	24000	45	0.78539816	0.018	3000000	5.5	0.6	110.518	156.295793	42
0.65	50000	0.5	24000	45	0.78539816	0.018	3000000	5.5	0.6	110.518	156.295793	43
0.65	50000	0.5	24000	45	0.78539816	0.018	3000000	5.5	0.6	110.518	156.295793	44
0.65	50000	0.5	24000	45	0.78539816	0.018	3000000	5.5	0.6	110.518	156.295793	45
0.65	50000	0.5	24000	45	0.78539816	0.018	3000000	5.5	0.6	110.518	156.295793	46
0.65	50000	0.5	24000	45	0.78539816	0.018	3000000	5.5	0.6	110.518	156.295793	47
0.65	50000	0.5	24000	45	0.78539816	0.018	3000000	5.5	0.6	110.518	156.295793	48
0.65	50000	0.5	24000	45	0.78539816	0.018	3000000	5.5	0.6	110.518	156.295793	49
0.65	50000	0.5	24000	45	0.78539816	0.018	3000000	5.5	0.6	110.518	156.295793	50

Model Spreadsheets

Conversion	Fb	solids, X	density, p	density, p	brookfield vis	brookfield vis	Variable B	Var. k	Var. gamma	min. CW	Model Formula	Mic.Set	Data
inch	lbs.	fractioned %	spec. grav.	lb/in^3	cP	lb/in·min							
0.001	0.15629579	0.6025	1.41	0.05091667	1220	0.06115421	0.0002155	0.5	5.1E-09	0	#NUM!	1	
0.002	0.31259159	0.6025	1.41	0.05091667	1220	0.06115421	0.0002155	0.5	5.1E-09	0	26.877	2	
0.003	0.46888738	0.6025	1.41	0.05091667	1220	0.06115421	0.0002155	0.5	5.1E-09	0	16.843	3	
0.004	0.62518317	0.6025	1.41	0.05091667	1220	0.06115421	0.0002155	0.5	5.1E-09	0	13.285	4	
0.005	0.78147897	0.6025	1.41	0.05091667	1220	0.06115421	0.0002155	0.5	5.1E-09	0	11.318	5	11
0.006	0.93777476	0.6025	1.41	0.05091667	1220	0.06115421	0.0002155	0.5	5.1E-09	0	10.026	6	
0.007	1.09407055	0.6025	1.41	0.05091667	1220	0.06115421	0.0002155	0.5	5.1E-09	0	9.095	7	
0.008	1.25036635	0.6025	1.41	0.05091667	1220	0.06115421	0.0002155	0.5	5.1E-09	0	8.383	8	
0.009	1.40666214	0.6025	1.41	0.05091667	1220	0.06115421	0.0002155	0.5	5.1E-09	0	7.816	9	
0.01	1.56295793	0.6025	1.41	0.05091667	1220	0.06115421	0.0002155	0.5	5.1E-09	0	7.350	10	6.96
0.011	1.71925373	0.6025	1.41	0.05091667	1220	0.06115421	0.0002155	0.5	5.1E-09	0	6.959	11	
0.012	1.87554952	0.6025	1.41	0.05091667	1220	0.06115421	0.0002155	0.5	5.1E-09	0	6.624	12	
0.013	2.03184531	0.6025	1.41	0.05091867	1220	0.06115421	0.0002155	0.5	5.1E-09	0	6.333	13	
0.014	2.18814111	0.6025	1.41	0.05091667	1220	0.06115421	0.0002155	0.5	5.1E-09	0	6.078	14	
0.015	2.3444369	0.6025	1.41	0.05091667	1220	0.06115421	0.0002155	0.5	5.1E-09	0	5.851	15	
0.018	2.50073269	0.6025	1.41	0.05091667	1220	0.06115421	0.0002155	0.5	5.1E-09	0	5.647	16	
0.017	2.65702849	0.6025	1.41	0.05091667	1220	0.06115421	0.0002155	0.5	5.1E-09	0	5.464	17	
0.018	2.81332428	0.6025	1.41	0.05091667	1220	0.06115421	0.0002155	0.5	5.1E-09	0	5.297	18	
0.019	2.96962007	0.6025	1.41	0.05091667	1220	0.06115421	0.0002155	0.5	5.1E-09	0	5.145	19	
0.02	3.12591588	0.6025	1.41	0.05091667	1220	0.06115421	0.0002155	0.5	5.1E-09	0	5.005	20	5.32
0.021	3.28221166	0.6025	1.41	0.05091667	1220	0.06115421	0.0002155	0.5	5.1E-09	0	4.876	21	
0.022	3.43850745	0.6025	1.41	0.05091867	1220	0.06115421	0.0002155	0.5	5.1E-09	0	4.757	22	
0.023	3.59480324	0.6025	1.41	0.05091667	1220	0.06115421	0.0002155	0.5	5.1E-09	0	4.645	23	
0.024	3.75109904	0.6025	1.41	0.05091667	1220	0.06115421	0.0002155	0.5	5.1E-09	0	4.542	24	
0.025	3.90739483	0.6025	1.41	0.05091667	1220	0.06115421	0.0002155	0.5	5.1E-09	0	4.445	25	
0.026	4.06369062	0.6025	1.41	0.05091667	1220	0.06115421	0.0002155	0.5	5.1E-09	0	4.353	26	
0.027	4.21998642	0.6025	1.41	0.05091667	1220	0.06115421	0.0002155	0.5	5.1E-09	0	4.268	27	
0.028	4.37628221	0.6025	1.41	0.05091667	1220	0.06115421	0.0002155	0.5	5.1E-09	0	4.187	28	
0.029	4.532578	0.6025	1.41	0.05091667	1220	0.06115421	0.0002155	0.5	5.1E-09	0	4.110	29	
0.03	4.6888738	0.6025	1.41	0.05091667	1220	0.06115421	0.0002155	0.5	5.1E-09	0	4.038	30	4.28
0.031	4.84516959	0.6025	1.41	0.05091667	1220	0.06115421	0.0002155	0.5	5.1E-09	0	3.969	31	
0.032	5.00146538	0.6025	1.41	0.05091667	1220	0.06115421	0.0002155	0.5	5.1E-09	0	3.904	32	
0.033	5.15776118	0.6025	1.41	0.05091667	1220	0.06115421	0.0002155	0.5	5.1E-09	0	3.842	33	
0.034	5.31405697	0.6025	1.41	0.05091667	1220	0.06115421	0.0002155	0.5	5.1E-09	0	3.783	34	
0.035	5.47035276	0.6025	1.41	0.05091667	1220	0.06115421	0.0002155	0.5	5.1E-09	0	3.726	35	
0.036	5.62664856	0.6025	1.41	0.05091867	1220	0.06115421	0.0002155	0.5	5.1E-09	0	3.672	36	
0.037	5.78294435	0.6025	1.41	0.05091667	1220	0.06115421	0.0002155	0.5	5.1E-09	0	3.620	37	
0.038	5.93924014	0.6025	1.41	0.05091667	1220	0.06115421	0.0002155	0.5	5.1E-09	0	3.570	38	
0.039	6.09553594	0.6025	1.41	0.05091667	1220	0.06115421	0.0002155	3.5	5.1E-09	0	3.522	39	
0.04	6.25183173	0.6025	1.41	0.05091667	1220	0.06115421	0.0002155	0.5	5.1E-09	0	3.477	40	
0.041	6.40812752	0.6025	1.41	0.05091667	1220	0.06115421	0.0002155	0.5	5.1E-09	0	3.432	41	
0.042	6.56442332	0.6025	1.41	0.05091667	1220	0.06115421	0.0002155	0.5	5.1E-09	0	3.390	42	
0.043	6.72071911	0.6025	1.41	0.05091667	1220	0.06115421	0.0002155	0.5	5.1E-09	0	3.349	43	
0.044	6.8770149	0.6025	1.41	0.05091667	1220	0.06115421	0.0002155	0.5	5.1E-09	0	3.310	44	
0.045	7.0333107	0.6025	1.41	0.05091667	1220	0.06115421	0.0002155	0.5	5.1E-09	0	3.271	45	
0.046	7.18960649	0.6025	1.41	0.05091667	1220	0.06115421	0.0002155	0.5	5.1E-09	0	3.235	46	
0.047	7.34590228	0.6025	1.41	0.05091667	1220	0.06115421	0.0002155	0.5	5.1E-09	0	3.199	47	
0.048	7.50219808	0.6025	1.41	0.05091667	1220	0.06115421	0.0002155	0.5	5.1E-09	0	3.164	48	
0.049	7.65849387	0.6025	1.41	0.05091667	1220	0.06115421	0.0002155	0.5	5.1E-09	0	3.131	49	
0.05	7.81478966	0.6025	1.41	0.05091667	1220	0.06115421	0.0002155	0.5	5.1E-09	0	3.099	50	

0.3 Extension Data

b roll-thick,t	roll elast. mo	poisson's ratio	velocity, U	angle	angle	blade thick, b	bl. elasilic mo	bl. width, W	extension, L	S	Final S	crometer Sett
inch	Er	v,	in./min	degrees	radians	inch	Eb	inch	inch		S/Cos(angle)	10^-6 Meters
0.65	50000	0.5	24000	45	0.78539816	0.018	3000000	5.5	0.3	838.945	1186.44689	1
0.65	50000	0.5	24000	45	0.78539816	0.018	3000000	5.5	0.3	838.945	1186.44689	2
0.65	50000	0 5	24000	45	0.78539816	0.018	3000000	5.5	0.3	838.945	1186.44689	3
0.65	50000	0.5	24000	45	0.78539816	0.018	3000000	5.5	0.3	838.945	1186.44689	4
0.65	50000	0.5	24000	45	0.78539816	0.018	3000000	5.5	0.3	838.945	1186.44689	5
0.65	50000	0.5	24000	45	0.78539816	0.018	3000000	5.5	0.3	838.945	1186.44689	6
0.65	50000	0.5	24000	45	0.78539816	0.018	3000000	5.5	0.3	838.945	1186.44689	7
0.65	50000	0.5	24000	45	0.78539816	0.018	3000000	5.5	0.3	838.945	1186.44689	8
0.65	50000	0.5	24000	45	0.78539816	0.018	3000000	5.5	0.3	838.945	1186.44689	9
0.65	50000	0.5	24000	45	0.78539816	0.018	3000000	5.5	0.3	838.945	1186.44689	10
0.65	50000	0.5	24000	45	0.78539816	0.018	3000000	5.5	0.3	838.945	1186.44689	11
0.65	50000	0.5	24000	45	0.78539816	0.018	3000000	5.5	0.3	838.945	1186.44689	12
0.65	50000	0.5	24000	45	0.78539816	0.018	3000000	5.5	0.3	838.945	1186.44689	13
0.65	50000	0.5	24000	45	0.78539816	0.018	3000000	5.5	0.3	838.945	1186.44689	14
0.65	50000	0.5	24000	45	0.78539816	0.018	3000000	5.5	0.3	838.945	1186.44689	15
0.65	50000	0.5	24000	45	0.78539816	0.018	3000000	5.5	0.3	838.945	1186.44689	16
0.65	50000	0.5	24000	45	0.78539816	0.018	3000000	5.5	0.3	838.945	1186.44689	17
0.65	50000	0.5	24000	45	0.78539816	0.018	3000000	5.5	0.3	838.945	1186.44689	18
0.65	50000	0.5	24000	45	0.78539816	0.018	3000000	5.5	0.3	838.945	1186.44689	19
0.65	50000	0.5	24000	45	0.78539816	0.018	3000000	5.5	0.3	838.945	1186.44689	20
0.65	50000	0.5	24000	45	0.78539816	0.018	3000000	5.5	0.3	838.945	1186.44689	21
0.65	50000	0.5	24000	45	0.78539816	0.018	3000000	5.5	0.3	838.945	1186.44689	22
0.65	50000	0.5	24000	45	0.78539816	0.018	3000000	5.5	0.3	838.945	1186.44689	23
0.65	50000	0.5	24000	45	0.78539816	0.018	3000000	5.5	0.3	838.945	1186.44689	24
0.65	50000	0.5	24000	45	0.78539816	0.018	3000000	5.5	0.3	838.945	1186.44689	25
0.65	50000	0.5	24000	45	0.78539816	0.018	3000000	5.5	0.3	838.945	1186.44689	26
0.65	50000	0.5	24000	45	0.78539816	0.018	3000000	5.5	0.3	838.945	1186.44689	27
0.65	50000	0.5	24000	45	0.78539816	0.018	3000000	5.5	0.3	838.945	1186.44689	28
0.65	50000	0.5	24000	45	0.78539816	0.018	3000000	5.5	0.3	838.945	1186.44689	29
0.65	50000	0.5	24000	45	0.78539816	0.018	3000000	5.5	0.3	838.945	1186.44689	30
0.65	50000	0.5	24000	45	0.78539816	0.018	3000000	5.5	0.3	838.945	1186.44689	31
0.65	50000	0.5	24000	45	0.78539816	0.018	3000000	5.5	0.3	838.945	1186.44689	32
0.65	50000	0.5	24000	45	0.78539816	0.018	3000000	5.5	0.3	838.945	1186.44689	33
0.65	50000	0.5	24000	45	0.78539816	0.018	3000000	5.5	0.3	838.945	1186.44689	34
0.65	50000	0.5	24000	45	0.78539816	0.018	3000000	5.5	0.3	838.945	1186.44689	35
0.65	50000	0.5	24000	45	0.78539816	0.018	3000000	5.5	0.3	838.945	1186.44889	36
0.65	50000	0.5	24000	45	0.78539816	0.018	3000000	5.5	0.3	838.945	1186.44689	37
0.65	50000	0.5	24000	45	0.78539816	0.018	3000000	5.5	0.3	838.945	1186.44689	38
0.65	50000	0.5	24000	45	0.78539816	0.018	3000000	5.5	0.3	838.945	1186.44689	39
0.65	50000	0.5	24000	45	0.78539816	0.018	3000000	5.5	0.3	838.945	1186.44689	40
0.65	50000	0.5	24000	45	0.78539816	0.018	3000000	5.5	0.3	838.945	1186.44689	41
0.65	50000	0.5	24000	45	0.78539816	0.018	3000000	5.5	0.3	838.945	1186.44689	42
0.65	50000	0.5	24000	45	0.78539816	0.018	3000000	5.5	0.3	838.945	1186.44689	43
0.65	50000	0.5	24000	45	0.78539816	0.018	3000000	5.5	0.3	838.945	1186.44689	44
0.65	50000	0.5	24000	45	0.78539816	0.018	3000000	5.5	0.3	838.945	1186.44689	45
0.65	50000	0.5	24000	45	0.78539816	0.018	3000000	5.5	0.3	838.945	1186.44689	46
0.65	50000	0.5	24000	45	0.78539816	0.018	3000000	5.5	0.3	838.945	1186.44689	47
0.65	50000	0.5	24000	45	0.78539816	0.018	3000000	5.5	0.3	838.945	1186.44689	48
0.65	50000	0.5	24000	45	0.78539816	0.018	3000000	5.5	0.3	838.945	1186.44689	49
0.65	50000	0.5	24000	45	0.78539816	0.018	3000000	5.5	0.3	838.945	1186.44689	50

0.3 Extension Data

Conversion inch	Fo lbs.	solids, X fractioned %	density, p spec. grav.	density, p lb/in^3	brookfield vis cP	brookfield vis lb/in·min	Variable B	Variable k	Var. gamma	Min. Ct. Wt.	Model Formula	Mic. Set	Data
0.001	1.18644689	0.6025	1.41	0.05091667	1220	0.06115421	0.0002155	0.5	5.1E-09	0	8.654	1	
0.002	2.37289378	0.6025	1.41	0.05091667	1220	0.06115421	0.0002155	0.5	5.1E-09	0	5.812	2	
0.003	3.55934068	0.6025	1.41	0.05091667	1220	0.06115421	0.0002155	0.5	5.1E-09	0	4.670	3	
0.004	4.74578757	0.6025	1.41	0.05091667	1220	0.06115421	0.0002155	0.5	5.1E-09	0	4.013	4	
0.005	5.93223446	0.6025	1.41	0.05091667	1220	0.06115421	0.0002155	0.5	5.1E-09	0	3.572	5	
0.006	7.11868135	0.6025	1.41	0.05091667	1220	0.06115421	0.0002155	0.5	5.1E-09	0	3.251	6	
0.007	8.30512824	0.6025	1.41	0.05091667	1220	0.06115421	0.0002155	0.5	5.1E-09	0	3.003	7	
0.008	9.49157513	0.6025	1.41	0.05091667	1220	0.06115421	0.0002155	0.5	5.1E-09	0	2.805	8	
0.009	10.678022	0.6025	1.41	0.05091667	1220	0.06115421	0.0002155	0.5	5.1E-09	0	2.641	9	
0.01	11.8644689	0.6025	1.41	0.05091667	1220	0.06115421	0.0002155	0.5	5.1E-09	0	2.503	10	4.25
0.011	13.0509158	0.6025	1.41	0.05091667	1220	0.06115421	0.0002155	0.5	5.1E-09	0	2.385	11	
0.012	14.2373627	0.6025	1.41	0.05091667	1220	0.06115421	0.0002155	0.5	5.1E-09	0	2.282	12	
0.013	15.4238096	0.6025	1.41	0.05091667	1220	0.06115421	0.0002155	0.5	5.1E-09	0	2.191	13	
0.014	16.6102565	0.6025	1.41	0.05091667	1220	0.06115421	0.0002155	0.5	5.1E-09	0	2.110	14	
0.015	17.7967034	0.6025	1.41	0.05091667	1220	0.06115421	0.0002155	0.5	5.1E-09	0	2.038	15	
0.016	18.9831503	0.6025	1.41	0.05091667	1220	0.06115421	0.0002155	0.5	5.1E-09	0	1.972	16	
0.017	20.1695972	0.6025	1.41	0.05091667	1220	0.06115421	0.0002155	0.5	5.1E-09	0	1.913	17	
0.018	21.3560441	0.6025	1.41	0.05091667	1220	0.06115421	0.0002155	0.5	5.1E-09	0	1.858	18	
0.019	22.5424909	0.6025	1.41	0.05091667	1220	0.06115421	0.0002155	0.5	5.1E-09	0	1.808	19	
0.02	23.7289378	0.6025	1.41	0.05091667	1220	0.06115421	0.0002155	0.5	5.1E-09	0	1.762	20	3.38
0.021	24.9153847	0.6025	1.41	0.05091667	1220	0.06115421	0.0002155	0.5	5.1E-09	0	1.719	21	
0.022	26.1018316	0.6025	1.41	0.05091667	1220	0.06115421	0.0002155	0.5	5.1E-09	0	1.679	22	
0.023	27.2882785	0.6025	1.41	0.05091667	1220	0.06115421	0.0002155	0.5	5.1E-09	0	1.642	23	
0.024	28.4747254	0.6025	1.41	0.05091667	1220	0.06115421	0.0002155	0.5	5.1E-09	0	1.607	24	
0.025	29.6611723	0.6025	1.41	0.05091667	1220	0.06115421	0.0002155	0.5	5.1E-09	0	1.575	25	
0.026	30.8476192	0.6025	1.41	0.05091667	1220	0.06115421	0.0002155	0.5	5.1E-09	0	1.544	26	
0.027	32.0340661	0.6025	1.41	0.05091667	1220	0.06115421	0.0002155	0.5	5.1E-09	0	1.515	27	
0.028	33.220513	0.6025	1.41	0.05091667	1220	0.06115421	0.0002155	0.5	5.1E-09	0	1.487	28	
0.029	34.4069599	0.6025	1.41	0.05091667	1220	0.06115421	0.0002155	0.5	5.1E-09	0	1.461	29	
0.03	35.5934068	0.6025	1.41	0.05091667	1220	0.06115421	0.0002155	0.5	5.1E-09	0	1.436	30	1.58
0.031	36.7798536	0.6025	1.41	0.05091667	1220	0.06115421	0.0002155	0.5	5.1E-09	0	1.413	31	
0.032	37.9663005	0.6025	1.41	0.05091667	1220	0.06115421	0.0002155	0.5	5.1E-09	0	1.391	32	
0.033	39.1527474	0.6025	1.41	0.05091667	1220	0.06115421	0.0002155	0.5	5.1E-09	0	1.369	33	
0.034	40.3391943	0.6025	1.41	0.05091667	1220	0.06115421	0.0002155	0.5	5.1E-09	0	1.349	34	
0.035	41.5256412	0.6025	1.41	0.05091667	1220	0.06115421	0.0002155	0.5	5.1E-09	0	1.329	35	
0.036	42.7120881	0.6025	1.41	0.05091667	1220	0.06115421	0.0002155	0.5	5.1E-09	0	1.311	36	
0.037	43.898535	0.6025	1.41	0.05091667	1220	0.06115421	0.0002155	0.5	5.1E-09	0	1.293	37	
0.038	45.0849819	0.6025	1.41	0.05091667	1220	0.06115421	0.0002155	0.5	5.1E-09	0	1.276	38	
0.039	46.2714288	0.6025	1.41	0.05091667	1220	0.06115421	0.0002155	0.5	5.1E-09	0	1.259	39	
0.04	47.4578757	0.6025	1.41	0.05091667	1220	0.06115421	0.0002155	0.5	5.1E-09	0	1.243	40	
0.041	48.6443226	0.6025	1.41	0.05091667	1220	0.06115421	0.0002155	0.5	5.1E-09	0	1.228	41	
0.042	49.8307695	0.6025	1.41	0.05091667	1220	0.06115421	0.0002155	0.5	5.1E-09	0	1.213	42	
0.043	51.0172163	0.6025	1.41	0.05091667	1220	0.06115421	0.0002155	0.5	5.1E-09	0	1.199	43	
0.044	52.2036632	0.6025	1.41	0.05091667	1220	0.06115421	0.0002155	0.5	5.1E-09	0	1.185	44	
0.045	53.3901101	0.6025	1.41	0.05091667	1220	0.06115421	0.0002155	0.5	5.1E-09	0	1.172	45	
0.046	54.576557	0.6025	1.41	0.05091667	1220	0.06115421	0.0002155	0.5	5.1E-09	0	1.159	46	
0.047	55.7630039	0.6025	1.41	0.05091667	1220	0.06115421	0.0002155	0.5	5.1E-09	0	1.146	47	
0.048	56.9494508	0.6025	1.41	0.05091667	1220	0.06115421	0.0002155	0.5	5.1E-09	0	1.134	48	
0.049	58.1358977	0.6025	1.41	0.05091667	1220	0.06115421	0.0002155	0.5	5.1E-09	0	1.123	49	
0.05	59.3223446	0.6025	1.41	0.05091667	1220	0.06115421	0.0002155	0.5	5.1E-09	0	1.111	50	1.14

Modeling Graph
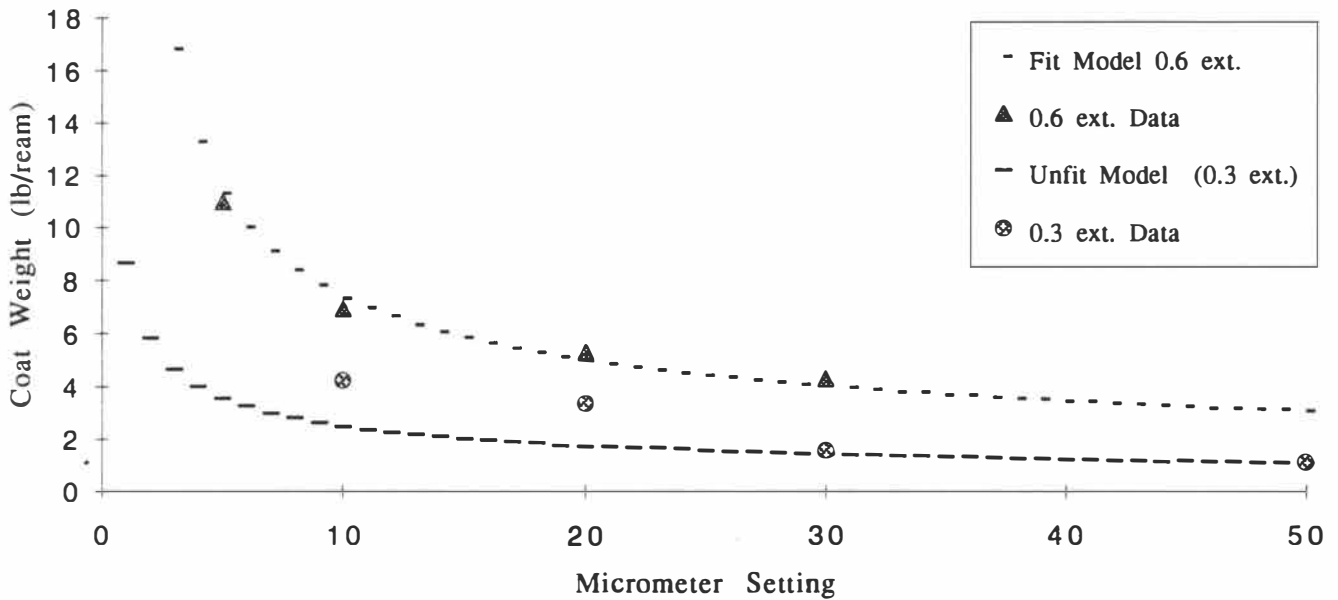
<u>0.6 Extension</u>
    1)   Fitted Equation
    2)   Original Trial Data

<u>0.3 Extension</u>
    1)   Predicted Equation
    2)   Original Trial Data

Model, Fitted 0.6 ext. & Plotted 0.3 ext.

RESULTS DISCUSSION

The model graph shows a very positive outcome. Numbers were generated for the fitted equation according to the information provided by Lyons (1993). After all the set values were entered, there were four variables to alter that would change the outcome of the model's values. Two of these variables, k and CW_O, were chosen to be set at 0.5 and 0, respectively. This allowed the other two, γ & β, to solely be the manipulators that would create the "fitted" values coinciding with the 0.6 extension original data. It is important to note that the micrometer setting was varied during the trial to obtain a range of coat weights. This had to be accounted for in the model spreadsheet as it influenced the stiffness and force values.

The method used to achieve the values was an iterative process. First, one variable was approximated, then the other was manipulated to find the best fit of the data points. Then once that was established, the first variable was altered to find a "best" fit. This method continued for a few times. Eventually, it led to difference comparisons of the original data coat weights to the model generated values at the corresponding run-in settings. Once these two numbers were found, a graph was created to visually demonstrate how well the fitted equation lined up with the actual data for that extension. The determined values for γ & β were then inputted on a separate spreadsheet for the 0.3 inch extension. The results were not manipulated, only plotted against the actual 0.3 inch coat weight data from the second trial run.

On the positive side, there was a good correlation of actual to modeling (or predicted) values for the high micrometer settings

using the 0.3 inch extension. The model's predictions for both 30 $\times 10^{-3}$ and 50 $\times 10^{-3}$ inch settings were accurate compared to the actual data. However, at lower settings, 10 $\times 10^{-3}$ and 20 $\times 10^{-3}$ inch, the predicted values were lower by a factor of two *(See RESULTS section model graph)*.

During the trial, there were some difficulties in obtaining accurate and consistent coat weight values. One large reason was the extremely stiff backing blade thickness, 0.25 inches, usually this is the same width as the coating blade (0.018), but it was suggested to use a thicker backer to constrain the geometeries more effectively. The backing blade is a piece of metal alloy that secures the coating blade into the process configuration. The distance from the backing blade's edge to the end of the coating blade is the blade extension.

This reason coupled with the low extension value of 0.3 inches, does not allow the system to give or flex under high blade forces, but rather it forces all deflections to occur over only the distance of the extension. It also allows a high amount of variance when lower blade forces are used, but lowers the variance under the higher blade forces defined as a more constrained system. Therefore, lower blade forces would actually allow more coating to slip through the blade because the sheet velocity would influence the coat weight determinations more.

There were other questionable parameters that may have influenced the trial results. First, the backing roll is known to expand from the heating stages of the trial. If it is not properly, pre-heated, after conducting a number of trials this expansion would increase and influence the results slightly. Therefore, for the most

part the expansion was accounted for by a number of "empty" runs before the first run producing system heat up for consistency. In addition, after changing the extension to start the second trial, the blade and micrometer were re-zeroed. This process also further stabilizes any backing roll expansion influence.

Second, the base paper's basis weight had a high degree of variation, +/- 2 lb/ream. This presented serious errors in the final coat weight calculations. To minimize this error, a number of averages were obtained. This definitely improved the results, but still produced significant errors in the original data.

Third, using the microwave to obtain final coat weights was utilized with speed in mind, however, it sacrifices accuracy because the power of the microwave may chemically alter the coating particles. If a starch had been used as a binder, there may have been a higher variation. A more precise method would have been an ash testing to find the exact amounts of coating applied. If the experiment were to be conducted again, it would be beneficial to make these adjustments.

An extremely good potential exists to conduct additional work in this model area. One possible benefit would be a computer program that could be developed to predict a range of micrometer settings to try to obtain a specific coat weight. Currently, this is accomplished by trial and error and operator experience. Since there is no production schedule to follow this is quite adequate, however, if production time loss was a serious factor to consider or if the paper substrate was either in short supply or extremely expensive, a computer model could optimize these factors.

Currently, this principle is far from implementation. There is no real account for different coating formulas. As shown by Roper and Attal (1993), different pigment and binder particles have different effects of coating rheology. This difference would certainly have an effect on the levels of the coating applied on the CLC. Numerous trials would need to be conducted to achieve various coat weights to narrow the system's uncertainty.

In addition, the entire model assumes no affect from different paper substrates. Therefore, if this parameter is changed a whole new set of trials must be conducted. The model does however factor out the different substrate influence, because it employs "fitted" to actual data comparison. As a result, the model would effectively work, but this limits the idea of a computer simulation program unless running specifically on the identical paper substrate.

In conclusion, the results correlated very positively with the expectations at high blade forces. Additional work on this modeling technique could eventually produce a useful tool for CLC trials. A various array of different blade extensions would secure better predictions.

CONCLUSIONS

- A positive correlation exists between actual data and modeling expectations.

- Highly constrained geometries (resulting from high run-in settings, hence high blade forces) show the best data correlations.

- It is quite possible to establish a computer simulation technique, but it would have to be paper substrate specific.

- Different coating formulations were not analyzed, so the technique might also have to coating formulation specific.

- There still exists numerous variables to control in future studies:
    Smaller Paper Substrate's Basis Weight Range of Variation
    Larger Blade Extensions: 0.4 to 0.7 inches
    Different Analysis of Coat Weight Determinations

RECOMMENDATIONS

Necessary Changes For Future CLC Modeling

- Different Extensions
    Ranging from 0.4 to 0.65

- Monitor the Backing Roll,
    Decrease Any Error Due To Expansion .

- Better Base Sheet
    Basis Weight Accuracy

- Test Method Comparison
    Ash Test Method To Microwave Method

- Use a Computer Modeling Program
    Determine Precise "Best Fit" Variables

- Make at Least 6 L of Coating
    Add Accurate Amounts of Thickener ("As Is" Basis)

- Find Possible Correlations to the Actual Model Equation
    Water Retention Test
    Capillary Shear Test
    Hercules High Shear Test

- Conduct Capillary Shear Test

Key Parameters To Stick With

- Completely Measure All Described Variables
    (See Procedure Section For List)

- Conduct Hercules High Shear Test

- Pre-Heat Backing Roll Before Starting Trials

Use the Stiff Backing Blade to Firmly Hold the Blade	OR	Account Movement from a Thinner, More Flexible Backing Blade

BIBLIOGRAPHY

1.   Roper, J. & Attal, J. (1993, May). Evaluations of Coating High-Speed Runnability Using Pilot Coater Data, Rheological Measurements, and Computer Modeling. Tappi Journal, 76 (5), 55-61.

2.   Triantafillopoulos, N. (1989). Measurement of Fluid Rheoloy and Interpretation of Rheograms. Kaltec Scinetific, Inc.

3.   Bliesner, W. C. (1971). Basic Mechanisms in Blade Coating. Tappi Journal, 54 (10). 1673-1679.

4.   Windle, W. & Beazley, K. M. (1967, January). The Mechanics of Blade Coating. Tappi Journal, (50)1, 1-7.

5.   Lyons, A. V. (1993, May 2). Mathematical Model of Coat Weight Control on the CLC. CLC User's Forum. Repap Technologies Inc.

6.   Gill, R. A. & Hagemeyer, R. W. (1994). Fillers For Paper. Paper Processes. (Vol 6, pp. 19-37). Atlanta: TAPPI Press.

7.   Sandas, S. E., Salminen, P. J., & Eklund, D. E. (1989, December). Measuring the Water Retention of Coating Colors. Tappi Journal, (72)12, 207-210.

8.   Branston R. E., Clark P. C., Errico M., Scriven L. E., Sheehan J. G., Suszynski W. J., Takamura K., & Vodnick J. L. (1994, January). Weeping in Blade Coating Tappi Journal, 77 (1). 131-138.

9.   Suwala, D. & Ottone, S. (1992, May). Parameter Design on the Cylindrical Laboratory Coater. Tappi Journal, 75 (5), 159-165.

ADDITIONAL READING MATERIAL

Clay

Johns, R., Berube, R., & Slepetys, R. (1990). Chemically Structured Kaolin: A New Coating Pigment. Tappi Journal, 73 (2). 77-81.

Hydrodynamic Theory

Scheller, B. L. & Bousfield, D. W. The Flow of Viscous Shear-Thinning Fluids in Narrow Geometries. Unpublished master's thesis, University of Maine, Orono, Maine.

Blade Coating

Eklund, D. & Salminen, P. J. (1986, January). Blade Coating Mechanics. Tappi Journal, (69)1, 112-117.

Follette, W. J. & Fowells, R. W. (1960, November). Operating Variables of a Blade Coater. Tappi Journal, (43)11, 953-957.

Bousfield, D. W. A Model to Predict the Leveling of Coating Defects. Tappi Journal, 74 (5), 163-170.

Water Retention of Coating

Herbert, A. J., Gautam, N., & Whalen-Shaw, M. J. (1990, November). A Simple Method for Measuring Immobilization Using the Surface Gloss Technique. Tappi Journal, (73)11, 167-174.

Engstrom, G., & Rigdahl, M. (1986, January). In-situ Studies of Water Drainage from Wet Coating Layers. Tappi Journal, (69)1, 86-89.

Chen, K. S. A., & Scriven, L. E. (1990, January). Liquid Penetration into a Deformable Porous Substrate. Tappi Journal, (73)1, 151-161.

Salminen, P. J. (1988, September). Water Transport into Paper- the Effect of Some Liquid and Paper Variables. Tappi Journal, (71)9, 195-199.

APPENDIX I

FIG 14

Water Retention Meter
for Accurate Measurement of Water Retention
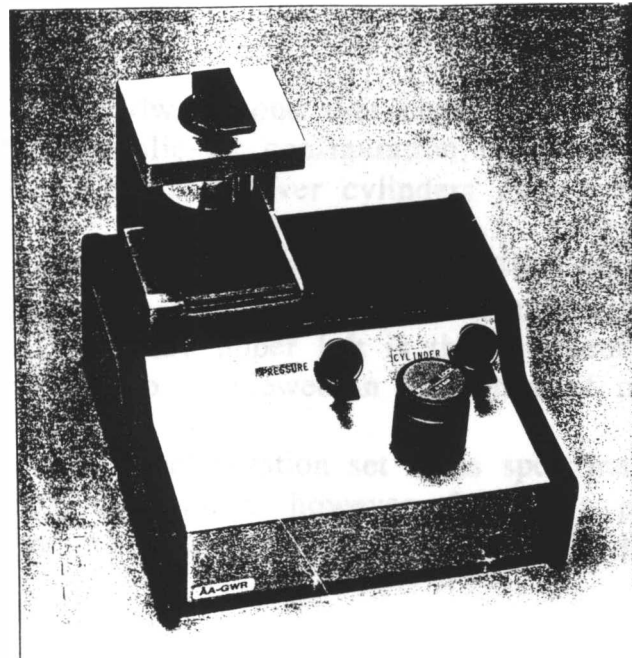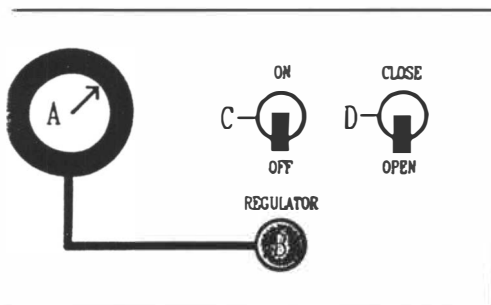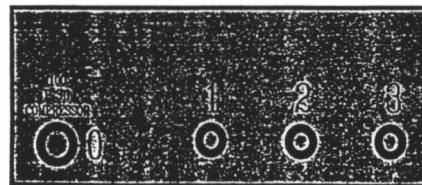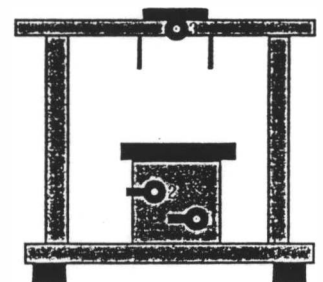

FIG. 15

BACK OF INSTRUMENT

0 = Compressed Air Inlet   1 = Cell Closed   2 = Cell Open
3 = Pressurize Measuring Cell
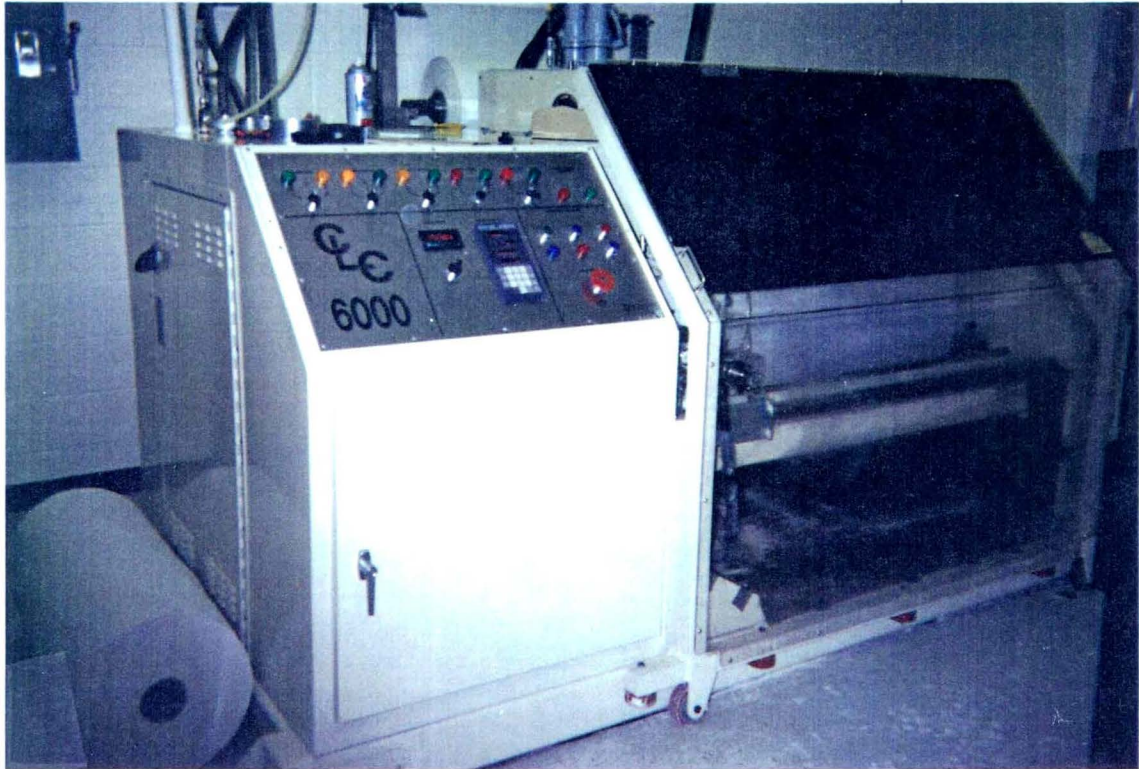
APPENDIX II

CLC Pictures

Picture 1 - The CLC ready for a trial run with the safety cover in place, seen as the black rectangle in the upper right that blocks most of the backing roll from view.

Picture 2 - The dwell pond that holds the coating suspension and the applicator configuration. The entire set up moves down the silver cylinders during a trial run.

This viewpoint is linearly **180°** opposite in respect to picture 1, the black cylinder to the right is the backing roll and in the upper left is the emergency stop button that can also be viewed in the center of picture 1.

This configuration set up is specifically for a roll coating application, however, from this perspective neither the blade nor roll could actually be viewed.